Digital holographic adaptive optics for ocular imaging: proof of principle

Changgeng Liu and Myung K. Kim*

Digital Holography and Microscopy Laboratory, Department of Physics, University of South Florida, Tampa, Florida 33620, USA
**Corresponding author: mkkim@usf.edu*

Received May 25, 2011; revised June 19, 2011; accepted June 21, 2011;
posted June 22, 2011 (Doc. ID 148228); published July 14, 2011

An adaptive optics (AO) ocular imaging system is proposed that is based on the principles of digital holography and dispenses with the wavefront sensor and wavefront modulator of conventional AO systems, thus reducing the optomechanical complexity and cost while increasing speed and resolution. Numerical simulations and proof-of-principle experiments are presented that demonstrate the feasibility. © 2011 Optical Society of America

OCIS codes: 010.1080, 330.4460, 170.4460.

Adaptive optics (AO), originally developed for astronomical telescopes, reduces the effect of atmospheric turbulence by measuring the distortion of the wavefront arriving from a point source (guide star) and using the information to compensate for the distortions in the objects to be imaged. When applied to ocular imaging, the guide star is provided by a narrow laser beam focused on a spot on the retina [1]. Most commonly, a Shack–Hartmann or pyramid wavefront sensor is used to measure the wavefront of the reflected light [2–4]. The wavefront distortion is then compensated for using a wavefront corrector, such as a deformable mirror or liquid crystal spatial light modulator [5,6]. The sensor and corrector typically have a few hundred elements, allowing for adjustment of a similar number of coefficients in the Zernike aberration polynomials. Several iterations of sensing, computation, and corrections are carried out in a feedback loop to reach a stable state. AO has been incorporated in scanning laser ophthalmoscopy [7], optical coherence tomography [8], and laser refractive surgery [9].

We propose an AO system that dispenses with the wavefront sensor and corrector. These are essential elements of current AO technology, but they are also the components that require a high degree of delicate alignment and maintenance, constraining the resolution, dynamic range, and speed, as well as driving up the cost. The system, named digital holographic AO (DHAO), is based on the ability of digital holography to quantitatively measure and numerically manipulate phase profiles of optical wavefronts [10–12]. It substantially reduces the complexity, and very likely the cost, of the optomechanical system. The wavefront sensing and correction by DHAO have almost the full resolution of the CCD camera [10–12]. It does not involve electronic–numerical–mechanical feedback. Numerical computation of holographic images is faster than the conventional AO feedback loop. The dynamic range of deformation measurement is essentially unlimited [12].

The principle of aberration compensation is a well-known characteristic of holography, as clearly demonstrated by Leith and Upatnieks in 1966 [13]. Numerical processing of the complex wavefronts measured by digital holography offers a new level of flexibility and versatility in sensing and control of aberration. Compensation of low-order aberrations, including tilt spherical aberration and astigmatism, have been demonstrated in digital holographic microscopy, either by double exposure of the field with and without the specimen or by assuming a portion of the object field to be flat [14]. Automatic compensation of higher order terms of the Zernike polynomials has been demonstrated and the concept of a numerical parametric lens has been introduced that can shift, magnify, and compensate for aberrations [15].

Below, we describe the principle of the proposed DHAO system. Numerical simulation examples are used to illustrate the DHAO process for the particular configuration appropriate for ocular imaging. Proof-of-principle experiments clearly demonstrate the feasibility to compensate for the ocular aberrations and significantly improve resolution in a robust and efficient manner.

The basic principle of DHAO is described using Fig. 1. It is a two exposure process. First, in Fig. 1(a), a narrow collimated laser beam enters the eye through the cornea and the lens of the eye, which forms a focused spot on the retina—the so-called "guide star." The diffraction-limited spot size is typically a few micrometers. The light scatters and reflects from the guide star spot and exits the eye with a broad coverage of the cornea and the lens, Fig. 1(b). Ideally, the emergent beam would be collimated and its wavefront planar, whereas any aberration of the eye's optics causes distortion of the wavefront. The phase profile of the wavefront is captured by digital holography and numerically stored, as described below in

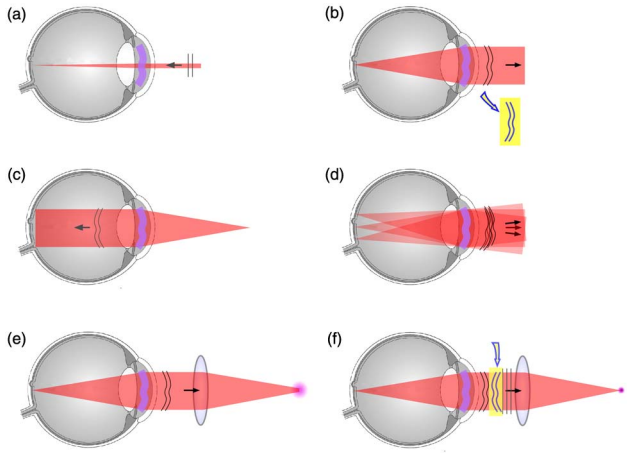

Fig. 1. (Color online) DHAO principle. See text for details.

the experimental section. In the second step, for full-field imaging of the retina, a focused source at the front focus of the eye lens results in a collimated illumination of the retina, Fig. 1(c). The illumination does contain phase distortion due to the eye's aberration, but this does not affect the final intensity image of the eye. The complex, i.e., amplitude and phase, optical field exiting the eye is again captured by digital holography at a plane in front of the cornea, Fig. 1(d). The captured complex optical field contains all the information necessary to reconstruct the image of the retina by using a numerical lens and numerically propagating an appropriate distance, Fig. 1(e). But the phase distortion degrades the point spread function of the resultant image, which can be compensated for by numerically subtracting the stored phase profile from the first step, Fig. 1(f). This description of DHAO assumes: (i) that the guide star input beam is narrow enough that the aberration across it is negligible, but large enough that the guide star spot is as small as possible compared to the retinal cell; and (ii) that most of the aberration is in the anterior region of the eye, i.e., the lens and the cornea, so that the aberration experienced by the light from various parts of the retina is approximately equal, see Fig. 1(d). Similar assumptions are necessary in conventional AO and they are not any more severe in DHAO.

The process of DHAO is illustrated using the simulation images in Fig. 2, where the retinal surface is represented with a resolution target pattern, Fig. 2(a). The field is assumed to be $2500\,\mu\text{m} \times 2500\,\mu\text{m}$ with 512 pixels× 512 pixels. (Note that the simulated pattern is *not* meant to be a correctly scaled copy of the United States Air Force (USAF) resolution target.) The retinal surface irregularity is represented with a random phase distribution of the retinal surface, Fig. 2(b). The eye is modeled to consist of a lens of focal length 25 mm and the retinal surface located at the focal plane of the lens. The lens is also assumed to contain an aberration in the form of a phase distortion corresponding to one of the Zernike polynomials $aZ_5^3(\rho,\varphi) = a(5\rho^5 - 4\rho^3)\cos 3\varphi$, defined on a circle of diameter $2500\,\mu$m and amplitude $a = 4\pi$, as depicted in Fig. 2(c). In sensing, the amplitude and phase profiles of the optical field emerging from a small area of the retina, i.e., the guide star, are shown in Figs. 1(d) and 1(e). It

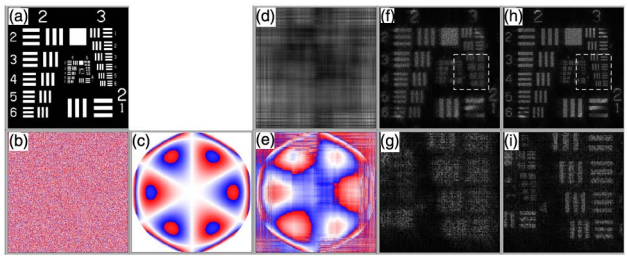

Fig. 2. (Color online) Simulation of DHAO process. Amplitude images are shown in gray scale and phase images [(b), (c), and (e)] in blue–white–red color scale, representing the range of phase from $-\pi$ to $+\pi$. (a) Assumed amplitude pattern on retina; (b) phase noise of retinal surface; (c) assumed aberration of the eye; (d) amplitude of exit field; (e) phase of exit field, representing measured aberration of the eye; (f) uncorrected image of retina and (g) its detail; and (h) corrected image of retina and (i) its detail.

is an approximate plane wave, with phase distortion due to the assumed aberration of the lens and the phase noise of the retina. For imaging, the light enters the eye lens, with aberration, and illuminates the retina, from which it reflects and exits the lens, again with the aberration. The emerging optical field is diffuse with random phase distribution, which can be captured in the experiment as a hologram. To reconstruct the image of the retina, one can simulate the propagation of light through an imaging lens (e.g., $f = 25\,\text{mm}$) and an appropriate distance ($z = 25\,\text{mm}$) to the image plane [12]. The resultant image is shown in Fig. 2(f) and a magnified view of the dotted square area is shown in Fig. 2(g). Now, in order to compensate for the aberration, the aberration field represented in Figs. 2(d) and 2(e) is conjugated and multiplied to the hologram before propagating through the imaging lens to the image plane. The result is shown in Fig. 2(h), and a magnified view of the dotted square area is shown in Fig. 2(i). Comparison of Figs. 2(f) and 2(h), or 2(g) and 2(i), clearly displays the feasibility of DHAO in resolution improvement.

The principle of DHAO is experimentally demonstrated using the apparatus shown in Fig. 3. First, a narrow collimated HeNe laser beam enters the eye and is focused on the retinal surface. For this proof-of-principle experiment, the eye is modeled by a combination of a simple lens ($f = 25\,\text{mm}$) (C) and a printed-on-paper resolution target (R) placed at the focal plane of the lens. The spot size on the retina is estimated to be $\sim 50\,\mu$m. The aberration of the eye is imitated by placing an irregular piece of glass (A) in front of the lens. The complex optical field of the emergent light is captured by the CCD camera, which is focused at the plane (H) through the relay lenses L2 and L3. The reference for the holographic imaging is provided by the beam splitter (BS1), the beam expander, and the beam combiner (BC). The reference is slightly tilted for off-axis holography configuration. For the full-field imaging of the retinal surface, another lens L1 is inserted so that its focus coincides with that of the eye lens, C. A second exposure of the hologram is acquired at the plane, H. The two holograms are numerically combined and processed as described above to finally obtain the aberration-compensated image of the retina. Thus, the same holographic interferometer serves to achieve the sensing of the aberration field and compensation of the aberration. In comparison with conventional AO, a lenslet array, a second CCD camera, and a deformable mirror are absent, significantly reducing the complexity and cost of the apparatus.

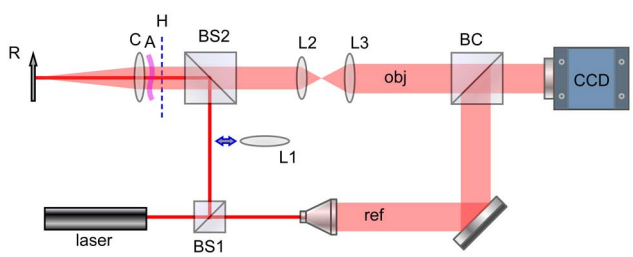

Fig. 3. (Color online) DHAO apparatus. The CCD camera plane is conjugate to the hologram plane H. R, retinal plane; C, corneal lens; A, aberrator. See text for details.

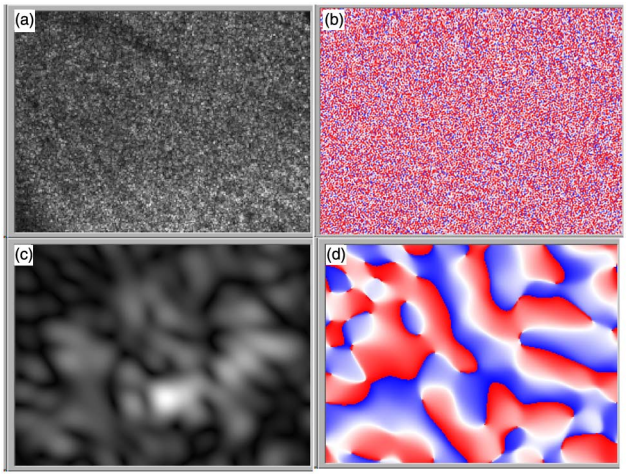

Fig. 4. (Color online) (a) Amplitude and (b) phase of complex hologram with full-field illumination. (c) Amplitude and (d) phase of complex hologram with guide star illumination. FOV is 2134 μm × 1601 μm.

Hologram images are shown in Fig. 4. The field of view (FOV) on the retinal plane is 2134 μm × 1601 μm with 1024 pixels × 768 pixels. The amplitude and phase of the complex hologram with full-field illumination is shown in Figs. 4(a) and 4(b). The complex hologram is obtained by taking the intensity hologram captured by the camera and numerically filtering one of the angular spectrum components [10–12]. The amplitude and phase of the complex hologram for guide star sensing is shown in Figs. 4(c) and 4(d).

The two holograms thus obtained are then used to reconstruct the retinal image. First, in Fig. 5(a), the image reconstructed from another hologram without the phase aberrator—the irregular piece of glass—in place is shown as a baseline. For reconstruction, we use a numerical lens of focal length 80 mm and the best image is obtained at a distance of 78 mm. The displayed image area corresponds to 1121 μm × 1121 μm on the retinal plane and shows the elements 3–5 of group 3 of the USAF resolution target. Then, Fig. 5(b) is the image reconstructed from the complex hologram of Figs. 4(a) and 4(b) without the aberration compensation, showing significant degradation of the resolution. Finally, in Fig. 5(c), the complex conjugate of the guide star hologram of Figs. 4(c) and 4(d) is multiplied to the uncorrected hologram of Figs. 4(a) and 4(b) before reconstruction. In both Figs. 5(b) and 5(c), the best focus images are obtained at a distance of 76 mm, the difference with the case of Fig. 5(a) being likely due to the presence of the piece of glass with approximately 1.2 mm thickness. The RMS deviation of the wavefront is determined from Fig. 4(d) to be 1.11 μm, a rather severe value compared to those expected in the normal population [1]. Compensation of the effect of the aberration and improvement of the resolution (better than ~40 μm) is quite evident, thus demonstrating the validity of the DHAO principle.

In summary, we have demonstrated the feasibility of the proposed DHAO system. Imaging experiments

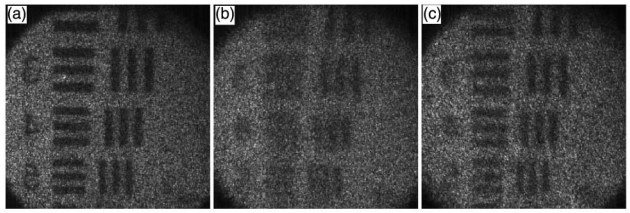

Fig. 5. Reconstructed images of the retinal plane (a) in the absence of an aberrator, (b) with an aberrator in place but without aberration correction, and (c) with an aberrator in place and after aberration correction. FOV is 1121 μm × 1121 μm.

using realistic eye models using human eye tissues are underway. A typical conventional AO system includes a spatial light modulator, a lenslet array, and a second CCD camera in addition to the camera for imaging. The proposed DHAO system replaces these hardware components with numerical processing for wavefront measurement and compensation of aberration through the principles of digital holography. The wavefront sensing and correction by DHAO have almost the full resolution of the CCD camera. It is inherently faster than conventional AO because it does not involve feedback and iteration, and the dynamic range of deformation measurement is essentially unlimited [12].

This work is supported in part by the National Science Foundation (NSF) grant No. 0755705.

References

1. K. M. Hampson, J. Mod. Opt. **55**, 3425 (2008).
2. J. Z. Liang, B. Grimm, S. Goelz, and J. F. Bille, J. Opt. Soc. Am. A **11**, 1949 (1994).
3. I. Iglesias, R. Ragazzoni, Y. Julien, and P. Artal, Opt. Express **10**, 419 (2002).
4. S. R. Chamot, C. Dainty, and S. Esposito, Opt. Express **14**, 518 (2006).
5. J. Liang, D. R. Williams, and D. Miller, J. Opt. Soc. Am. A **14**, 2884 (1997).
6. Q. Mu, Z. Cao, D. Li, L. Hu, and L. Xuan, Opt. Express **15**, 1946 (2007).
7. A. Roorda, F. Romero-Borja, W. J. Donnelly III, H. Queener, T. J. Herbert, and M. C. W. Campbell, Opt. Express **10**, 405 (2002).
8. R. J. Zawadzki, S. S. Choi, A. R. Fuller, J. W. Evans, B. Hamann, and J. S. Werner, Opt. Express **17**, 4084 (2009).
9. T. Kohnen, J. Buhren, C. Kuhne, and A. Mirshahi, Ophthalmol. annu. **111**, 2175 (2004).
10. E. Cuche, P. Marquet, and C. Depeursinge, Opt. Lett. **24**, 291 (1999).
11. C. Mann, L. Yu, C. Lo, and M. K. Kim, Opt. Express **13**, 8693 (2005).
12. M. K. Kim, SPIE Reviews **1**, 018005 (2010).
13. J. Upatnieks, A. V. Lugt, and E. N. Leith, Appl. Opt. **5**, 589 (1966).
14. L. Miccio, D. Alfieri, S. Grilli, P. Ferraro, A. Finizio, L. De Petrocellis, and S. D. Nicola, Appl. Phys. Lett. **90**, 041104 (2007).
15. T. Colomb, F. Montfort, J. Kuhn, N. Aspert, E. Cuche, A. Marian, F. Charriere, S. Bourquin, P. Marquet, and C. Depeursinge, J. Opt. Soc. Am. A **23**, 3177 (2006).